Mouse intraflagellar transport proteins regulate both the activator and repressor functions of Gli transcription factors

Aimin Liu[1], Baolin Wang[2] and Lee A. Niswander[1,*,†]

[1]Department of Pediatrics, University of Colorado at Denver and Health Sciences Center, Mailstop 8322, Box 6511, Aurora, CO 80045, USA
[2]Department of Genetic Medicine, Cornell University Weill College of Medicine, New York, NY 10021,USA
*Howard Hughes Medical Institute investigator
†Author for correspondence (e-mail: lee.niswander@uchsc.edu)

Accepted 27 April 2005

Development 132, 3103-3111
Published by The Company of Biologists 2005
doi:10.1242/dev.01894

Summary

Intraflagellar transport (IFT) is an active event in which cargo is transported along microtubules by motor proteins such as kinesin and dynein. IFT proteins are required for the formation and maintenance of flagella and cilia. We have previously shown that mouse mutants for two IFT proteins, IFT88 and IFT172, as well as Kif3a, a subunit of mouse kinesin 2, exhibit ventral spinal cord patterning defects that appear to result from reduced hedgehog (Hh) signaling. Although genetic epistasis experiments place IFT proteins downstream of the Hh receptor and upstream of the Gli transcription factors, the mechanism by which IFT regulates Gli function is unknown.

The developing limb provides an excellent system to study Hh signaling, in particular as it allows a biological and molecular readout of both Gli activator and repressor function. Here we report that homozygous mutants for flexo (*Fxo*), a hypomorphic allele of mouse IFT88 generated in our ENU mutagenesis screen, exhibit polydactyly in all four limbs. Molecular analysis indicates that expression domains of multiple posteriorly restricted genes are expanded anteriorly in the mutant limbs, similar to loss of Gli3 transcriptional repressor function. Sonic hedgehog (*Shh*) expression is normal, yet *Ptch1* and *Gli1*, two known targets of Hh signaling, are greatly reduced, consistent with loss of Shh signaling. Expression of *Gli3* and *Hand2* in the mutant limb indicates that the limb prepattern is abnormal. In addition, we show that partial loss-of-function mutations in another mouse IFT gene, *Ift52* (*Ngd5*), result in similar phenotypes and abnormal Hh signaling as *Fxo*, indicating a general requirement for IFT proteins in Hh signaling and patterning of multiple organs. Analysis of *Ift88* and *Shh* double mutants indicates that, in mouse, IFT proteins are required for both Gli activator and repressor functions, and Gli proteins are insensitive to Hh ligand in the absence of IFT proteins. Finally, our biochemical studies demonstrate that IFT proteins are required for proteolytic processing of Gli3 in mouse embryos. In summary, our results indicate that IFT function is crucial in the control of both the positive and negative transcriptional activities of Gli proteins, and essential for Hh ligand-induced signaling cascade.

Key words: IFT88 (TTC10), IFT52, Gli, Hh signaling

Introduction

The Hedgehog (Hh) family of secreted proteins play important roles in regulating growth and patterning in both invertebrate and vertebrate animals (Ingham and McMahon, 2001). In mammalian embryos, Hh proteins are required for normal development of numerous organ systems. Loss of Hh function results in defects in almost every aspect of mouse embryogenesis, including loss of left-right asymmetry, dorsalization of the central nervous system (CNS) and a great reduction in digit number (Chiang et al., 1996). Hh proteins are also important survival factors and/or mitogens for multiple cell types, and unregulated activation of Hh signaling is implicated in the formation of various tumors (Bak et al., 2003).

Despite extensive studies of the Hh pathway, the transduction and regulation of Hh signaling in vertebrate has yet to be fully understood (Lum and Beachy, 2004). In *Drosophila*, Hh protein binds and inactivates its receptor Patched (Ptc), allowing the activation of Smoothened (Smo), another transmembrane protein. The principal target of Hh signaling is the transcription factor Cubitus interruptus (Ci). In the absence of Hh signaling, Ci is proteolytically processed into a transcriptional repressor, whereas Hh signaling inhibits such processing and allows the unprocessed Ci to act as a transcriptional activator. In the mouse, homologues for some major components of Hh signaling have been isolated and exhibit conserved functions in Hh signaling. However, important divergence exists between the Hh signaling pathway in insects and in vertebrates. First, owing to gene duplication, there are three Hh proteins (Shh, Ihh and Dhh) and three Ci homologues (Gli1, Gli2 and Gli3) in the mouse. Among the three Gli proteins, Gli1 does not contain a repressor domain and cannot be proteolytically processed, and thus appears to be an obligate activator (Dai et al., 1999). Gli2 and Gli3 contain both repressor and activator domains (Dai et al., 1999; Sasaki et al., 1999). Gli3 can be processed into transcriptional

repressors in vivo (Wang et al., 2000), although it remains to be determined whether Gli2 is processed in vivo. However, both biochemical and genetic evidence indicates that Gli3 predominantly acts as a repressor and Gli2 predominantly as an activator (Ding et al., 1998; Hui and Joyner, 1993; Matise et al., 1998). Furthermore, novel regulators of Hh signaling that appear to be specific to vertebrates have been isolated, suggesting that vertebrates have evolved different mechanisms to regulate Hh activity (Chuang and McMahon, 1999; Huangfu et al., 2003; Izraeli et al., 1999; Lee et al., 2001; McCarthy et al., 2002). This paper focuses on two novel regulators, both IFT proteins, to elucidate the molecular mechanisms underlying their regulation of Hh signal transduction.

The pattern of vertebrate limbs along the anteroposterior axis and formation of digits are regulated by the interaction between sonic hedgehog (Shh) and Gli3 (Niswander, 2003). *Shh* is expressed in a small group of mesenchymal cells in the posterior distal region of the early limb bud (the zone of polarizing activity, ZPA). Application of either ZPA cells or Shh protein to the anterior region of the limb bud leads to the formation of extra digits (polydactyly) in chick and mouse (Liu et al., 1998; Riddle et al., 1993). By contrast, all digits but one are lost in the absence of Shh protein function, reflecting the requirement for Shh function in digit formation (Chiang et al., 1996). Conversely, loss of Gli3 function as found in the mouse mutant *extra-toes* results in the formation of multiple digits and there is ectopic *Shh* expression in the anterior region of the limb bud (Buscher et al., 1997; Hui and Joyner, 1993). Ectopic Hh activity, or loss of Gli3 repressor function, has also been observed in several other mouse and chicken mutants with polydactyly (Wang et al., 2000; Yang et al., 1998). Interestingly, in the absence of Shh and Gli3 function, skeletal formation is rescued and multiple digits are formed although they are unpatterned (Litingtung et al., 2002; te Welscher et al., 2002b). From this, it has been concluded that Shh-Gli3 interactions serve to control the number and pattern of the digits.

Intraflagellar transport (IFT) proteins are required for the biogenesis of flagella and cilia in multiple organisms, including the green alga *Chlamydomonas reinhardtii*, *C. elegans*, insects and mouse (Rosenbaum and Witman, 2002). We have previously shown that in the mouse spinal cord, mutations in two IFT proteins, IFT88 (TTC10 – Mouse Genome Informatics) and IFT172, lead to loss of several ventral cell types and reduced expression of the Hh downstream gene *Ptch1* (Huangfu et al., 2003). However, the ventral defects in these mutants are not as severe as those in *Shh* or *Smo* mutants, raising the issue of whether these IFT proteins are essential components of the Hh pathway. In addition, these IFT mutants die around E10.5, preventing more thorough analysis of Hh signaling in other organs, especially in the limb where requirement for the repressor function of Gli proteins can be better addressed. *Orpk*, an existing hypomorphic allele of mouse *Ift88*, survives to young adulthood with multiple defects, including an extra thumb and polycystic kidneys (Moyer et al., 1994). However, it has been reported that Hh signaling and anteroposterior patterning gene expression is normal in *Orpk* limbs except for an anterior expansion of *Fgf4* expression in the apical ectodermal ridge (AER) (Zhang et al., 2003).

In this report, we show that flexo, a novel hypomorphic mutant of mouse IFT88, forms multiple digits in all four limbs despite the lack of ectopic Hh signaling and the downregulation of Hh activity in its normal domain. Hypomorphic mutants for another mouse IFT gene, *Ift52*, exhibit similar phenotypes to flexo mice in multiple organs. We also show, by double mutant analysis, that IFT proteins are required for tissues to respond to Hh ligand. Finally, we show that IFT proteins regulate Gli activity in part through the proteolytic processing of the Gli3 protein. Thus, IFT protein function is required for both the activator and repressor activities of the Gli proteins in the Hh pathway.

Materials and methods

Generation and genotyping of mutant mice

The generation and genotyping of $Ift88^{null}$ and $Ift88^{hypo}$ are as described previously (Huangfu et al., 2003). cDNA sequence of mouse *Ngd5* gene (*Ift52* homolog; Genbank Accession Number L38481) was used to Blast against Bay Genomics database (http://baygenomics.ucsf.edu/). Two gene-trap ES cell clones, XL826 and RRJ295, were identified to carry mutations in *Ngd5* genes. The $Ift52^{hypo}$ mice were generated by blastocyst injection of these ES cells and kept on C3H background. Mice carrying these mutations were genotyped by PCR using *lacZ*-specific primers (Liu et al., 1999) or MIT markers (D2mit49 and D2mit226) flanking the IFT52 gene. *Ptch1-lacZ* and *Shh* mutant mice are genotyped as described (Goodrich et al., 1997; Chiang et al., 1996).

Tissue processing and histochemistry

Whole-mount RNA in situ hybridization on embryos was performed as described (Liu et al., 1998). Immunohistochemical study on frozen cryosectioned tissue was performed as described (Timmer et al., 2001).

Western blot

Protein lysate was prepared from E10.5 wild type, $Gli3^{-/-}$, $Ift88^{null}$ $Ift88^{hypo}$ or $Ift52^{hypo}$ mouse whole embryo, dissected spinal cord or limb buds. Equal amounts of protein were loaded onto 7% SDS-PAGE gels and western blotting was performed as described (Wang et al., 2000). Anti β-tubulin antibody (Sigma, #T4026) was used as loading control. The result of western blot was quantitated using NIH Image 1.60.

Results

$Ift88^{hypo}$ limbs exhibit polydactyly and anterior expansion of posterior genes

Flexo (*Fxo*) is a recessive mouse mutation that causes multiple defects, including defects in dorsoventral patterning of the CNS (see Fig. 4) and polydactyly (6-9 digits) in all four limbs (Fig. 1A-D). Sequence analysis of DNA from *Fxo* embryos indicates that a splice mutation in mouse *Ift88* leads to a 29 amino acid deletion in the IFT88 protein (Huangfu et al., 2003). However, a normal *Ift88* transcript is detected at very low level and shortened cilia are detected in ventral node cells (data not shown). The similar but milder phenotype observed in *Fxo* mutant embryos relative to *Ift88*-null embryos indicates *Fxo* is a hypomorphic allele of *Ift88* (also Fig. 7 for more evidence). In order to avoid unnecessary confusion, we refer to the *Fxo* allele as $Ift88^{hypo}$ and to the null allele as $Ift88^{null}$.

$Ift88^{hypo}$ mutants survive until E12.5, allowing us to examine anteroposterior patterning in the $Ift88^{hypo}$ limb bud. Normally, *Fgf4* is expressed in the posterior aspect of the AER at E10.5 (Fig. 1E) and begins to be downregulated at E11.5 (Niswander and Martin, 1992). We found that *Fgf4* expression in $Ift88^{hypo}$

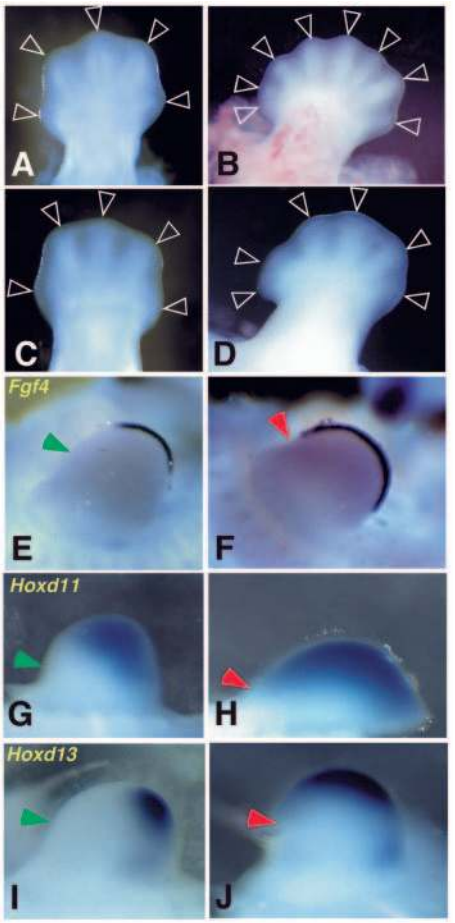

Fig. 1. *Ift88*^{hypo} limbs exhibit polydactyly and anterior expansion of posterior genes. (A,C) Normal forelimb (A) and hindlimb (C) bud at E12.5 with five digits; (B,D) *Ift88*^{hypo} forelimb (B) and hindlimb (D) bud at E12.5 show polydactyly. Arrowheads indicate digit condensations. (E) *Fgf4* is normally expressed in the posterior AER; (F) *Fgf4* is expressed in the entire AER of *Ift88*^{hypo} mutant limb bud at E10.5. (G,I) *Hoxd11* (G) and *Hoxd13* (I) are normally expressed in the posterodistal mesenchyme of E10.5 limb; (H,J) in *Ift88*^{hypo} mutants, *Hoxd11* (H) and *Hoxd13* (J) expression is expanded anteriorly and proximally. Green and red arrowheads in E-J indicate the anterior boundary of the AER in wild-type and *Ift88*^{hypo} limbs, respectively.

embryos is expanded to the entire length of AER at E10.5 (Fig. 1F) and its expression is maintained at E11.5 in the anterior AER (data not shown). Homeobox genes *Hoxd11* and *Hoxd13* are both normally expressed in the posterior mesenchyme of the limb buds at E10.5 and E11.5 (Fig. 1G,I; data not shown), and ectopic expression of Hoxd genes in the anterior parts of the limb has been shown to cause polydactyly and homeotic transformation (Knezevic et al., 1997; Morgan et al., 1992). We found that both genes are expressed in an expanded region at both E10.5 and E11.5 (Fig. 1H,J; data not shown). Therefore, the formation of extra digits in the limb coincides with an anterior-to-posterior transformation.

Hh signaling and limb prepattern is defective in *Ift88*^{hypo} mutant limbs

Hh signaling is required for maintaining posterior genes such as *Fgf4*, *Hoxd11* and *Hoxd13*, and plays essential roles in digit formation (Chiang et al., 2001; Kraus et al., 2001). Ectopic *Hh* expression and/or Hh activity revealed by Hh target gene expression such as *Ptch1* and *Gli1*, has been found to be associated with polydactyly as well as ectopic *Fgf4* and *Hoxd* expression in mouse and chick (Hui and Joyner, 1993; Yang et al., 1998). We therefore examined whether the polydactyly phenotype in *Ift88*^{hypo} limbs is associated with ectopic expression of *Shh* and *Ptch1*. In mutant limbs at both E10.5 and E11.5, there is no ectopic *Shh* expression and *Shh* is expressed normally in the posterior mesenchyme (Fig. 2A,B; data not shown). There is also no ectopic *Ptch1* expression in *Ift88*^{hypo} limbs (Fig. 2C,D; data not shown). Therefore, the formation of extra digits does not appear to correlate with ectopic *Hh* expression or activity. Surprisingly, the endogenous *Ptch1* expression is greatly reduced, at both E10.5 and E11.5 (Fig. 2C,D and data not shown). *Gli1* is another target gene of Hh signaling and its expression appears to depend strictly on Hh signaling (Bai et al., 2004). *Gli1* expression in *Ift88*^{hypo} limb is also downregulated at E10.5 (Fig. 2E,F). Thus, although *Shh* is normally expressed, there appears to be a loss of Hh signal transduction in the *Ift88*^{hypo} mutant limb bud.

It has been suggested that a mutual repression between *Gli3* and *Hand2* in the early limb buds sets up a limb prepattern that determines the anteroposterior polarity of the limb (te Welscher et al., 2002a). This prepattern exists before *Shh* expression initiates in the limb and hence is not affected by a mutation in the *Shh* gene (Chiang et al., 2001). We therefore examined the expression of *Hand2* and *Gli3* at E10.25 and E10.5 to determine whether the limb prepattern is altered in *Ift88*^{hypo} limbs. Normally, *Hand2* is expressed in the posterior mesenchyme of the early and later limb buds (Fig. 2G,I). In *Ift88*^{hypo} limbs, *Hand2* expression is both upregulated and anteriorly expanded (Fig. 2H,J). This suggests that the limb prepatterning defect results from a failure of Gli3 to repress *Hand2* expression; however, *Gli3* RNA is present in *Ift88*^{hypo} limbs (Fig. 2K-N). Later, *Gli3* expression expands posteriorly (Fig. 2N), which is probably due, in part, to the loss of Shh signaling. Taken together with the data above, the analysis of *Ift88*^{hypo} limbs indicates loss of both Gli activator function (downregulation of *Ptch1* and *Gli1* expression) and Gli repressor function (*Hand2* misexpression and polydactyly).

Ift52 mutants display similar embryonic defects as *Ift88*^{hypo} mutants

Our results that both Hh signaling and limb patterning along the anteroposterior axis are altered in *Ift88*^{hypo} mutants are in contrast to a previous report in which there was no change detected in the expression patterns of *Shh*, *Ptch1* or *Hoxd* genes in limbs of another hypomorphic allele of mouse *Ift88, Orpk* (Zhang et al., 2003). In contrast to *Ift88*^{hypo}, the *Orpk* mutant mice can survive to postnatal stage and the polydactyly phenotype is much milder than *Ift88*^{hypo} (Moyer et al., 1994). Therefore, it is possible that an alteration in gene expression would be too mild to detect in the *Orpk* mutant embryos.

Ift88^{hypo} is so far the only mouse IFT mutant to survive long enough to reveal the role for IFT88 in the regulation of both activator and repressor functions of Gli proteins. In order to determine whether the phenotype seen in *Ift88*^{hypo} reflects a general requirement for IFT proteins in Gli-positive and -negative regulation, we sought additional IFT mutant alleles

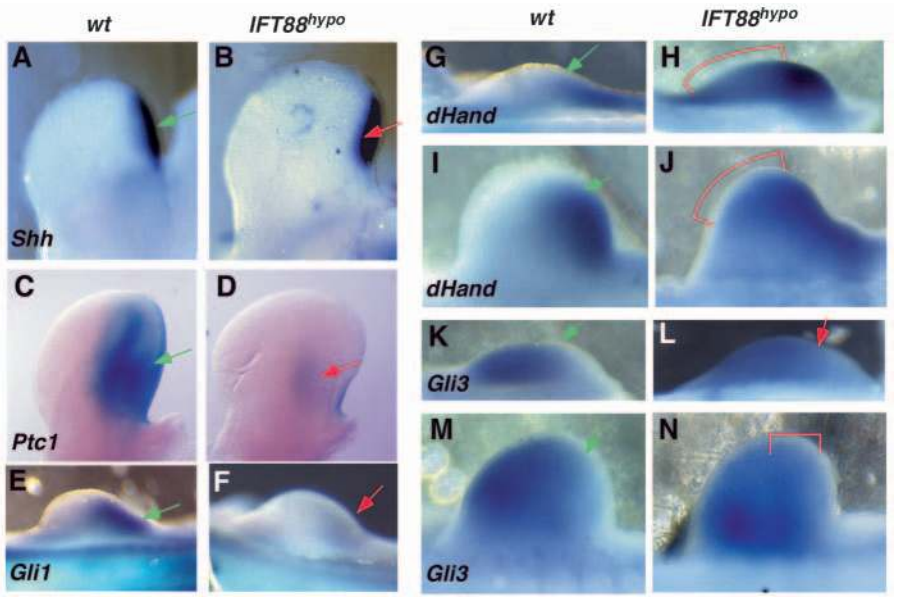

Fig. 2. Hh signaling and limb prepattern is defective in *Ift88*^{hypo} mutant limbs. (A,B) E10.5 forelimbs. (A) *Shh* is expressed in the posterior mesenchyme in wild-type limbs at E10.5. (B) *Shh* expression is normal in *Ift88*^{hypo} limbs. (C) *Ptch1-lacZ* is strongly expressed in cells adjacent to the *Shh* expression domain in wild-type E11.5 limbs. (D) *Ptch1-lacZ* (Goodrich et al., 1997) is expressed at very low levels in *Ift88*^{hypo} E11.5 limbs. (E,F) E10.5 hind limbs. (E) *Gli1* is expressed in the posterior region of the wild-type limb bud at E10.5. (F) *Gli1* expression is downregulated in *Ift88*^{hypo} limbs at E10.5; (G,I) *Hand2* (*dHand* in figure) is expressed in the posterior region of the wild-type limb bud at E10.25 and E10.5, respectively; (H,J) *Hand2* expression is upregulated and anteriorly expanded in *Ift88*^{hypo} limbs at both E10.25 and E10.5. (K,M) Gli3 RNA is expressed throughout the wild-type limb bud, except in the most posterior domain at E10.25 and E10.5. (L,N) In *Ift88*^{hypo} limbs at E10.25, *Gli3* is expressed as in wild type, but later expands into the posterior mesenchyme. Green arrows indicate gene expression in normal limbs; red arrows indicate gene expression in *Ift88*^{hypo} limbs; brackets indicate gene expression in *Ift88*^{hypo} limbs.

that allow a characterization of both CNS and limb development.

Mouse *Ngd5* shares sequence homology with *Chlamydomonas Ift52* (Wick et al., 1995) (data not shown). In addition, Ngd5 protein physically interacts with other known mammalian IFT proteins, indicating that it is the mammalian ortholog of IFT52 (Baker et al., 2003). Using a Blast search, we identified two ES cell lines (Bay Genomics) in which the *Ngd5* gene is disrupted by insertion of the *lacZ* sequence. In the first line (XL826), the C-terminal 99 amino acids of Ngd5 protein are replaced with *lacZ* sequence, whereas in the second allele (RRJ295), the last 47 amino acids are replaced with *lacZ* (Fig. 3A). We derived mutant embryos from both mutant ES cell lines and they both exhibited similar defects in embryogenesis. Therefore, we refer to both lines as *Ift52*^{hypo}.

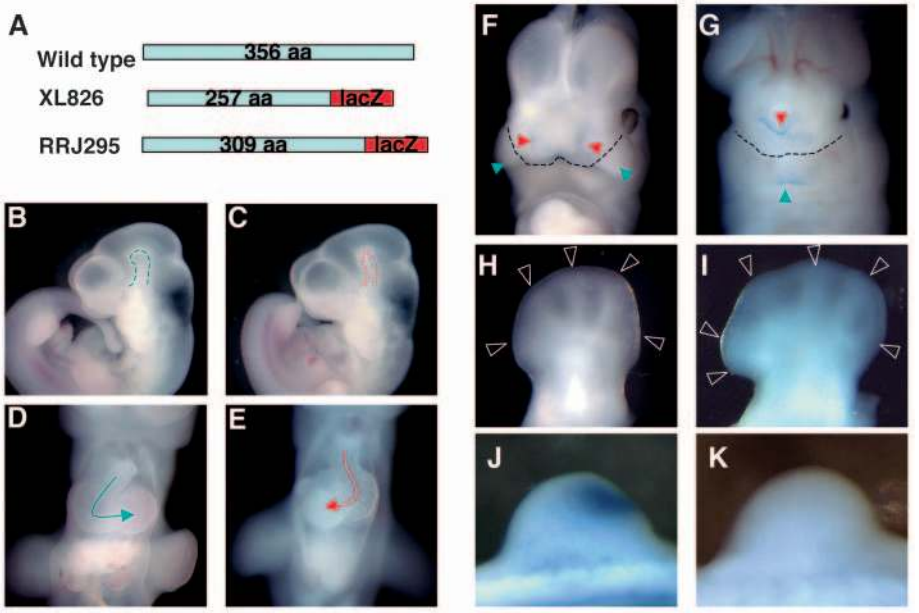

Fig. 3. Loss of IFT52 function leads to multiple defects in embryogenesis. (A) Wild type IFT52 encodes for a protein of 356 amino acids. In the first mutant line (XL826), the N-terminal 257 amino acids of IFT52 are fused to β-galactosidase protein. In the second mutant line (RRJ295), the N-terminal 309 amino acids of IFT52 are fused to β-galactosidase protein. (B) A wild-type E10.5 embryo has round smooth mesencephalic flexure (outlined). (C) An *Ift52*^{hypo} E10.5 embryo has tight mesencephalic flexure (outlined). (D) The heart tube in wild-type embryo loops to the left. (E) The heart tube in *Ift52*^{hypo} loops to the right. (F) The left and right olfactory pits (red arrowheads) and maxillary arches (blue arrowheads) are separated at E10.5 in wild-type embryos but are fused in the ventral midline in *Ift52*^{hypo} E10.5 embryos (G). Broken lines in F,G outline the ventral boundaries of the mandibular processes. (H) A limb bud of wild-type E12.5 embryo with five digits (white arrowheads). (I) A limb bud of *Ift52*^{hypo} mutant with six digits (white arrowheads). (J) *Ptch1* expression in an E10.5 wild-type limb bud. (K) *Ptch1* expression is not detectable in an E10.5 *Ift52*^{hypo} limb bud.

At E10.5, homozygous *Ift52*^{hypo} mutants have a tighter mesencephalic flexure compared with their wild-type littermates (Fig. 3B,C) and/or a neural tube closure defect (Fig. 3G). In wild-type embryos, the heart tube always loops to the left (Fig. 3D), whereas about half of the *Ift52*^{hypo} homozygous mutant embryos display right-looping heart tubes, indicating defects in left-right axis determination (Fig. 3E). Craniofacial development is also abnormal in *Ift52*^{hypo} mutant embryos. At E10.5, normal mouse embryos have separated olfactory pits and maxillary arches (red and blue arrowheads, respectively, in Fig. 3F). By contrast, in the E10.5 *Ift52*^{hypo} mutant embryos both the olfactory pits and maxillary arches are fused at the ventral midline (red and blue arrowhead,

respectively in Fig. 3G). At E12.5, polydactyly (6-7 digits) is seen in all four limbs (Fig. 3H,I). As *Ptch1* expression is downregulated in *Ift88*^{hypo} limb buds, indicating defective Hh signaling, we examined whether similar downregulation also occurs in *Ift52*^{hypo} limb buds. *Ptch1*, which is normally expressed in the posterodistal region of the limb buds at E10.5 (Fig. 3J), is not expressed in the *Ift52*^{hypo} limb buds (Fig. 3K), indicating IFT52 is also required for Hh signaling.

The tight mesencephalic flexure, left-right and ventral midline defects as well as polydactyly seen in *Ift52*^{hypo} embryos are very similar to what is seen in *Ift88*^{hypo} embryos. Loss of *Ptch1* expression in the *Ift52*^{hypo} limb buds further indicates that, similar to IFT88, IFT52 is also required for normal Hh signaling. We therefore examined ventral patterning of the spinal cord in both *Ift52*^{hypo} and *Ift88*^{hypo} mutant embryos. Our published studies of *Ift88* null mutants (*Ift88*^{null}) show that the floorplate, V3 interneurons and motoneurons are all absent (Huangfu et al., 2003). In *Ift88*^{hypo} and *Ift52*^{hypo} mutant spinal cord, *Shh*-expression in the floor plate is absent (Fig. 4A,E,I). *Nkx2.2*-expressing cells that give rise to V3 interneurons and that are normally dorsal and lateral to floorplate (Fig. 4B) are still present in the mutants, but they occupy the ventral most region of the spinal cord and the number is greatly reduced (Fig. 4F,J). Motoneurons that express *Isl1/2* are normally located dorsally to V3 interneurons (Fig. 4C); in the two hypomorphic IFT mutants, these cells expand into more ventral regions (Fig. 4G,K). Interestingly, scattered motoneurons are found in the ventral midline of the spinal cord, presumably among V3 interneurons. *Pax6* is normally strongly expressed in motoneuron precursors and weakly expressed in more dorsal regions of the spinal cord (Fig. 4D). In the two mutants, *Pax6* is ectopically expressed in scattered cells in more ventral regions of the spinal cord (Fig. 4H,L). Therefore, both *Ift88*^{hypo} and *Ift52*^{hypo} mutant embryos exhibit similar defects in ventral patterning of the spinal cord, and this phenotype is consistent with compromised Hh signaling.

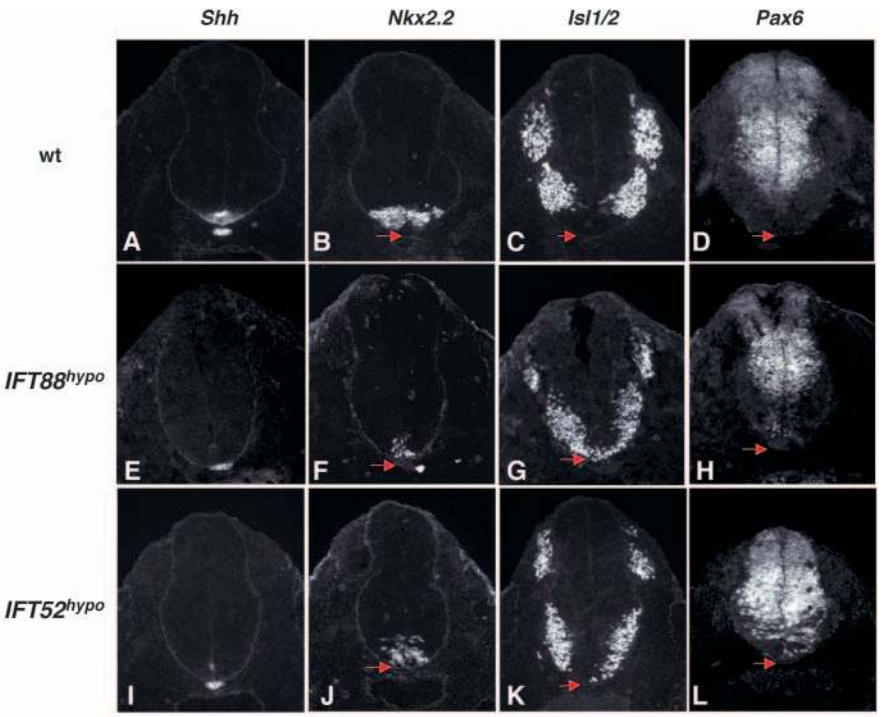

Fig. 4. Both *Ift88*^{hypo} and *Ift52*^{hypo} mutant embryos have ventral spinal cord defects. (A-D) In the wild-type spinal cord, (A) *Shh* is expressed in both the notochord and floorplate, (B) *Nkx2.2*-expressing cells are adjacent to the floor plate, (C) *Isl1/2*-expressing motoneurons are dorsal to *Nkx2.2* cells, and (D) *Pax6* is expressed weakly in dorsal neural progenitors and strongly in the intermediate regions in the spinal cord. (E-L) In both IFT mutants (E,I), the *Shh* expression in the floorplate is absent, (F,J) a reduced number of *Nkx2.2* expressing cells are present in the ventral midline of the spinal cord, (G,K) *Isl1/2*-expressing cells are found scattered in the ventral midline, and (H,L) cells strongly expressing *Pax6* are found scattered ectopically in the ventral most region of the spinal cord. Red arrows indicate the ventral most part of the spinal cord.

IFT88 is essential for Hh signaling

In order to further address the relationship between IFT proteins and Hh signaling, we characterized the double mutant between *Ift88* and *Shh*. *Ift88*^{null} mutants have defects in ventral spinal cord patterning that is similar to *Shh* mutants. However, interesting differences exist between the two mutants. In *Shh* mutants, the spinal cord is severely dorsalized. *Pax7*, which labels the dorsal progenitor cells, is expanded throughout the entire spinal cord (Fig. 5A,B). Strong *Pax6* expression, which labels neural progenitor cells in the ventral-intermediate region of the spinal cord, is shifted to the ventral most part of the spinal cord (Fig. 5E,F). *Lhx3* is normally expressed in both motoneurons and V2 interneurons, and *En1* is expressed in differentiated V1 interneurons that are dorsally adjacent to V2 interneurons (Fig. 5I,M). In *Shh* mutants, very few *En1*- and *Lhx3*-expressing cells are present in the ventral midline of the spinal cord (Fig. 5J,N). By contrast, in the *Ift88*^{null} spinal cord, *Pax7* expression remains dorsally restricted (Fig. 5C). Strong *Pax6* expression is detected in a broader domain expanded both ventrally and dorsally (Fig. 5G). *En1*- and *Lhx3*-expressing cells are both present but expanded to the ventral midline (Fig. 5K,O). One interpretation for the apparent milder ventral defects in *Ift88*^{null} is that Hh can partially signal through Gli in the absence of IFT88, which would predict that loss of Hh ligand in addition to IFT88 leads to a severe dorsalizing defect similar to that seen in *Shh* mutants. We hence generated double *Ift88*^{null}; *Shh*$^{-/-}$ mutant embryos to determine whether this is indeed the case.

In the spinal cord of the double homozygous mutants between *Ift88*^{null} and *Shh* (*Ift88*^{null}; *Shh*$^{-/-}$), *Pax7* expression is dorsally restricted (Fig. 5D) and *Pax6* is strongly expressed in most of the spinal cord, except for the most dorsal region, where it is expressed at a lower level (Fig. 5H). *En1*- and *Lhx3*-positive cells are present and expanded into the ventral midline (Fig. 5L,P). These patterns of expression of spinal cord neural progenitor and differentiated cell markers resemble that in

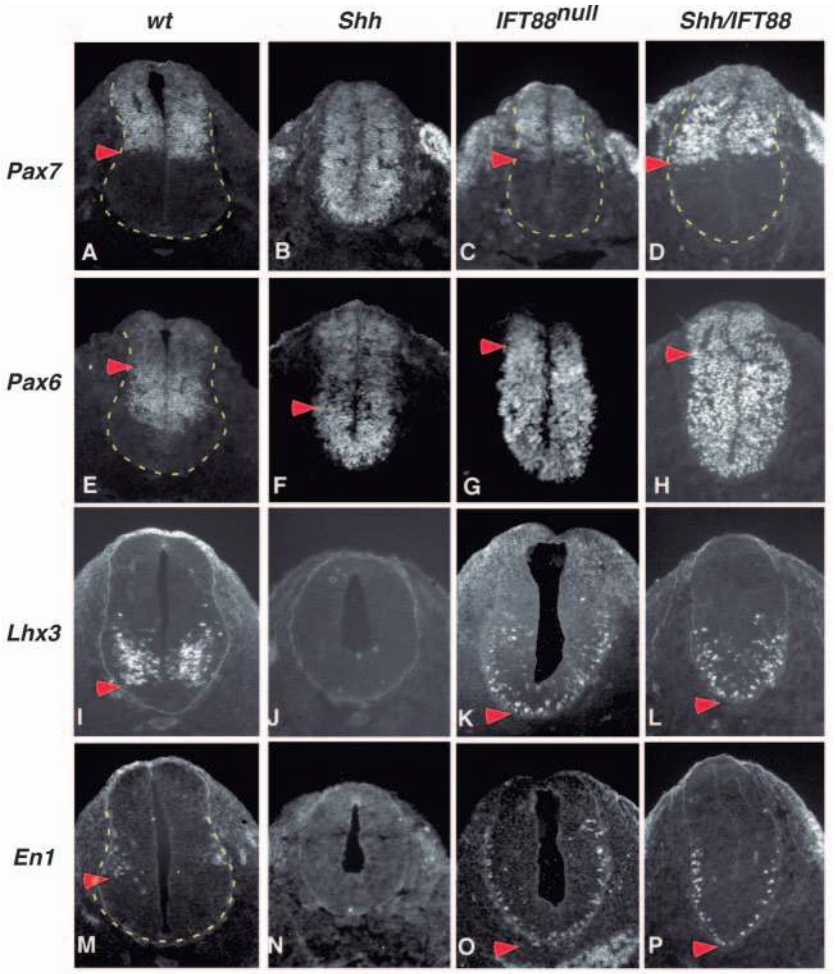

Fig. 5. IFT88 is essential for Hh signaling in the spinal cord. (A) *Pax7* is expressed in the dorsal neural progenitors in the spinal cord in normal embryos. (B) *Pax7* is expressed in the entire spinal cord, except for the most dorsal part in *Shh* mutants. (C) *Pax7* expression remains dorsally restricted in *Ift88*^{null} mutant (C) and in *Shh/Ift88*^{null} double mutant (D) spinal cord. (E) *Pax6* is weakly expressed in the dorsal spinal cord and strongly expressed in the intermediate region in wild-type embryos. (F) Strong *Pax6* expression is shifted to the ventral most region of the spinal cord in *Shh* mutants. (G) Strong *Pax6* expression is expanded to the ventral region of the spinal cord in *Ift88*^{null}. It also appears to be expanded more dorsally. (H) Strong *Pax6* expression appears to be expanded both dorsally and ventrally in *Shh/Ift88*^{null} double mutants. (I) *Lhx3* is expressed in differentiated motoneurons and V2 interneurons in normal embryos. (J) No or few *Lhx3*-expressing cells are present in ventral midline of *Shh* mutant spinal cord. (K,L) *Lhx3* expression is expanded to the ventral midline of the spinal cord in *Ift88*^{null} (K) and *Shh/Ift88*^{null} double mutants (L). (M) *En1*-expressing V1 interneurons are dorsally adjacent to V2 interneurons in normal embryos. (N) There are no or very few *En1*-expressing cells present in the ventral midline of the *Shh* mutant spinal cord. (O,P) *En1* expression is expanded to the ventral midline of the spinal cord in both *Ift88*^{null} (O) and *Shh/Ift88*^{null} mutant (P) embryos. Broken yellow lines outline the spinal cord. Arrowheads in A,C,D indicate the ventral border of the *Pax7* expression domains. Arrowheads in E-H indicate the boundary between the dorsal weak *Pax6* domain and the strong *Pax6* domains. Arrowhead in I,K,L and M,O,P indicate the ventral border of the expression domains of *Lhx3* and *En1*, respectively.

Ift88^{null} mutants, indicating that IFT88 is epistatic to Shh and it is an essential regulator of Hh signaling or Gli function. It has been suggested that severe ventral spinal cord patterning defects in *Shh* mutants may result from unregulated Gli3 repressor function (Litingtung and Chiang, 2000). Therefore, a more plausible interpretation for the *Ift88*^{null} spinal cord phenotype is that there is a loss of both Gli activator and repressor function. Indeed, when all Gli activities are ablated in mouse embryos, the dorsoventral patterning of the spinal cord is similar to that in *Ift88*^{null} embryos (Bai et al., 2004). Thus, we suggest that in *Shh* mutants, Gli3 repressor function remains active leading to a severe patterning defect, whereas in *Ift88*^{null}, *Ift88*^{hypo} and *Ift52*^{hypo} mutants, there is a loss of both Gli activator and repressor functions leading to less severe patterning defects.

Ift88^{hypo} mutation rescues limb formation in *Shh* mutants

The double mutants between *Shh* and *Ift88*^{null} die around E10.5. Therefore, in order to address the relationship between IFT proteins and Hh signaling during limb patterning, we generated double mutants between *Shh* and *Ift88*^{hypo}. At E12.5, *Shh* embryos are smaller than their littermates and exhibit severe midline defects with the loss of most craniofacial structures replaced with a proboscis-like structure and a cyclopic eye (Fig. 6A) (Chiang et al., 1996). The double mutants between *Shh* and *Ift88*^{hypo} are of normal size, and some of the craniofacial structures are restored and the two eyes are separated by midline tissue (Fig. 6B; data not shown). The general morphology of the double mutants is similar to *Ift88*^{hypo} single mutants (Fig. 6C), consistent with our observation in the spinal cord of *Shh/Ift88*^{null} double mutants.

It has been shown that anteroposterior patterning and formation of digits in the mammalian limbs depends on the interaction between Shh and Gli transcription factors, mainly Gli3 (Niswander, 2003), and that the major function of Shh in the limb is likely to antagonize the repressive function of Gli3 (Litingtung et al., 2002; te Welscher et al., 2002b). In E12.5 *Shh* mutant limbs, the posterior tissue degenerates, leaving a narrow pointy bud with a single digit condensation (Fig. 6D) (Chiang et al., 2001; Kraus et al., 2001). By contrast, the *Shh/Ift88*^{hypo} double mutants display polydactyly (Fig. 6E), similar to *Ift88*^{hypo} mutants (Fig. 6F). Moreover, the polydactyly is similar to that observed following loss of Gli3. In the absence of *Gli3*, multiple digits are formed, with the anterior expansion of otherwise posteriorly located genes such as *Fgf4*, *Hoxd11* and *Hoxd13* (Buscher et al., 1997; Hui and Joyner, 1993). *Ift88*^{hypo} mutant limb buds also display an anterior expansion of *Fgf4*, *Hoxd11* and *Hoxd13*, along with the formation of extra digits, suggesting a loss of *Gli3* repressor function. The fact that the polydactyly of *Ift88*^{hypo} mutants is not altered by loss of Shh function also suggests that there is

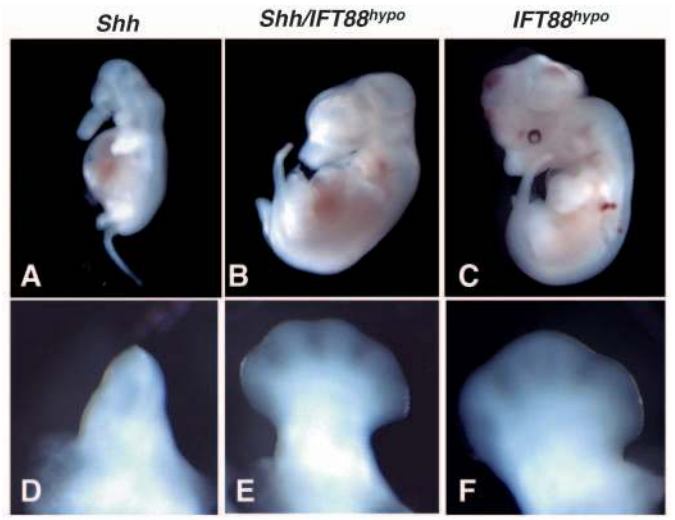

Fig. 6. Mutation in IFT88 rescues limb formation in *Shh* mutants. (A) At E12.5, *Shh* mutant embryos are smaller and have a cyclopic eye, proboscis-like facial structure and curly tail. (B) *Shh/Ift88*^{hypo} double mutants are of normal size, have separated eyes, partially rescued facial structure and normal looking tail. (C) *Ift88*^{hypo} embryos have very mild ventral midline defects and sometimes exencephaly. (D) *Shh* mutant embryos have only one digit in all four limbs. (E) *Shh/Ift88*^{hypo} double mutant limbs and (F) *Ift88* ^{hypo} mutant limbs display multiple digits.

a loss of Gli3 repressor function in *Ift88*^{hypo} mutants. However, the loss of the Shh targets *Ptch1* and *Gli1* in both the limb and other places in *Ift88*^{hypo} embryos, but not *Gli3* mutant embryos, also indicate a loss of Gli activator functions. The simplest explanation for such paradoxical phenotype is that IFT proteins are required, independently of Hh input, for both the activator and repressor function of Gli transcription factors.

IFT proteins regulate Gli proteolytic processing

To address directly the question of how IFT proteins may regulate the Gli transcriptional activities at molecular level, we examined whether mutations in IFT genes affect Gli3 protein processing. We performed western blot analysis using an antibody against the N terminus of Gli3 that recognizes both the Gli3 activator and repressor forms (Wang et al., 2000). In E10.5 wild-type whole embryos, most full-length Gli3 protein (Gli3-190) is proteolytically processed into the repressor form Gli3-83, and the amount of Gli3-190 is minimal (Fig. 7A, lane 1). By contrast, in *Ift88*^{null} mutants, the amount of processed Gli3 is significantly reduced as the full-length protein is dramatically increased (Fig. 7A, lane 2). As a result, the ratio of Gli3-190 versus Gli3-83 is markedly increased in the *Ift88*^{null} mutant embryos when compared with that in wild type (1.13 to 0.39) (Fig. 7B). Interestingly, although Gli3 processing was also disrupted in *Ift88*^{hypo} mutant embryos (Fig. 7, compare lane 3 with lane 4), the quantitative analysis revealed that *Ift88*^{hypo} mutation has less effect on Gli3 processing than *Ift88*^{null} mutation does, as measured by the ratio of Gli3-190 to Gli3-83 (Fig. 7B). Similar results were obtained in *Ift52*^{hypo} mutant embryos at the same stage (data not shown), indicating that the severity of the mutant phenotype correlates well with the defects in Gli3 processing. We also examined the extent of Gli3 processing in spinal cord and limb buds and found a similar accumulation of Gli3-190 and a reduction of Gli3-83 (data not shown), indicating that IFT proteins are essential for regulating Gli3 processing in diverse tissues. Our results in three different mutants strongly suggest that IFT regulates Gli3 at a step prior to its proteolysis. It is of note that, despite the accumulation of Gli3 full-length proteins, the IFT mutant embryos lack the molecular and embryological hallmarks of Gli activator function, indicating the full-length Gli proteins present in the mutants lack the ability to fully activate downstream genes.

Discussion

Our analysis indicates that newly synthesized, unmodified Gli proteins do not possess full transcriptional activities. IFT proteins, directly or indirectly, modify the Gli proteins (perhaps by targeting them to the appropriate location in the cell for modification), allowing them to acquire full transcriptional activity. Such modification by IFTs also primes the Gli proteins for further processing through proteolytic cleavage to generate Gli repressors. This proteolytic processing is negatively regulated by Hh. The modified Gli proteins, either the activator or the repressor, are then transported to the nucleus to regulate gene transcription. A novel gene, *iguana*, has been identified in zebrafish to regulate the nuclear import of Gli proteins (Sekimizu et al., 2004; Wolff et al., 2004). Our results have not addressed the possibility of an additional role for IFT proteins at this important step. Thus, in the absence of IFT function, Gli

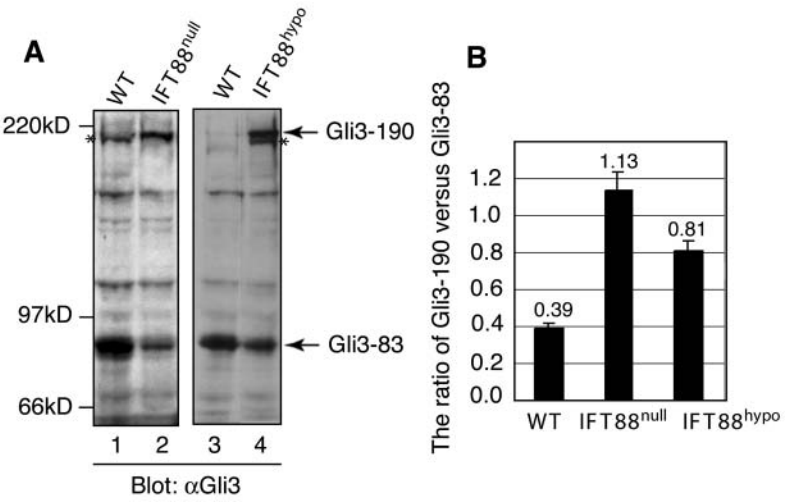

Fig. 7. IFT88 mutations affect Gli3 processing. (A) Immunoblots show the levels of Gli3-190 and Gli3-83 in wild type, *Ift88*^{null} and *Ift88*^{hypo} mouse embryos at E10.5. In wild-type embryos, the majority of Gli3 protein is proteolytically processed to form Gli3-83, whereas in both *Ift88*^{null} and *Ift88*^{hypo} mutants, the Gli3 processing is impaired. The bands marked with asterisks in lanes 1 and 4 are nonspecific and not consistently detectable. (B) Graphical representation of the ratio of Gli3-190 versus Gli3-83 in wild type, *Ift88*^{null} and *Ift88*^{hypo} mutant embryos. The results were obtained from three independent experiments. Numbers above the bars show an average of the ratio.

proteins lack the modifications that are crucial for their activator and repressor activities, as well as their competence to respond to Hh signaling.

In *Drosophila*, *Costal 2* (*Cos2*) and *Fused* (*Fu*) appear to play similar bipartite roles in Hh signaling such that both gain and loss of Hh signaling phenotypes are observed in such mutants (Lefers et al., 2001; Wang and Holmgren, 2000). *Cos2*, a Kinesin II-related protein without a functional motor, seems to play multiple roles in Hh signaling, including recruiting Ci to the cell surface through Smo and cytoplasmic retention of Ci (Jia et al., 2003; Lum et al., 2003; Ogden et al., 2003; Ruel et al., 2003; Wang and Holmgren, 2000). Fu is a Kinase whose only function appears to be antagonizing the function of Sufu, a negative regulator of Ci. Interestingly, when Fu is mutated, Ci cleavage is blocked and full-length Ci accumulates in the cells (Lefers et al., 2001).

Hh signaling in vertebrates appears to be more complex than that in insects. First, three Gli family members play different roles in mediating Hh signals, whereas in *Drosophila* there is only a single Ci gene that encodes both an activator and a repressor. Second, the existence and function of Cos2 and Fu in the vertebrate has yet to be confirmed. Third, IFT proteins that are crucial for mouse Hh signaling do not appear to mediate Hh signaling in *Drosophila* (Han et al., 2003; Sarpal et al., 2003). Therefore, vertebrates may use different sets of proteins to regulate Gli3 processing and subcellular localization of Gli proteins. Finally, as the loss of IFT functions leads to simultaneous loss of cilia and abnormal Hh signaling, it is difficult to distinguish a more direct function of IFTs as a component of the Hh pathway in the regulation of Gli protein modification, or a more indirect function, through signals associated with cilia.

Despite the divergence on the molecules involved, the vertebrate and insects may share similar strategy in regulating Gli/Ci activities. Kif3a, a subunit of mouse kinesin 2, plays important roles in Hh signaling (Huangfu et al., 2003). Although Kif3a does not seem to be the mouse ortholog of Cos2 according to sequence homology, it may be functionally equivalent. IFT proteins may also be a novel addition to the Gli-Kinesin (Ci-Cos2) complex that serves to bring Gli proteins to Smo upon activation of the pathway similar to what has been shown in *Drosophila* (Jia et al., 2003; Lum et al., 2003; Ogden et al., 2003; Ruel et al., 2003; Wang and Holmgren, 2000). It will be interesting in the future to elucidate whether a functional relationship exists between these proteins, and to determine the subcellular site(s) of IFT action and their interacting protein partners.

In summary, we have shown that IFT proteins are required for the proteolytic processing of Gli3 protein. Although there is an increase in the ratio of full-length activator to repressor Gli3 protein forms, this is not reflected genetically as the IFT mutants lack the hallmarks of in vivo Gli activator functions. Our analysis of two novel IFT mutants, as well as double mutants for *Ift88* and *Shh*, demonstrate that Gli activator as well as Gli repressor functions are disrupted and that IFT is an essential component of the Hh signaling pathway. Thus, IFT proteins are required for both the activator and repressor functions of Gli transcription factors.

We thank Dr P. Beachy for *Shh* mutant mice and Dr M. Scott for the *Ptc-lacZ* mice. For in situ probes, we thank Dr D. Duboule for *Hoxd11* and *Hoxd13*, Dr K. Ligon for *Hand2*, and Dr A. Joyner for *Gli1* and *Gli3*. We are grateful to the MSKCC Mouse Transgenic Core Facility for the blastocyst injections. We thank Drs J. Hooper, L. Sussel and I. Zohn for critically reading the manuscript. Monoclonal antibodies against Shh, Isl1/2, Nkx2.2 (developed by Jessell), Pax6 and Pax7 (developed by Kawakami) were obtained from Developmental Studies Hybridoma Bank developed under the auspices of the NICHD and maintained by the University of Iowa. The ES cell lines used to generate *Ift52* mutant mice are from Bay Genomics. This work was supported by a fellowship from NICHD to A.L. (F32-HD045090), an NIH grant to B.W. (R01 CA111673) and an NIH grant to L.A.N. (RO1 HD32427). L.A.N. is a HHMI investigator.

References

Bai, C. B., Stephen, D. and Joyner, A. L. (2004). All mouse ventral spinal cord patterning by hedgehog is Gli dependent and involves an activator function of Gli3. *Dev. Cell* **6**, 103-115.

Bak, M., Hansen, C., Tommerup, N. and Larsen, L. A. (2003). The Hedgehog signaling pathway – implications for drug targets in cancer and neurodegenerative disorders. *Pharmacogenomics* **4**, 411-429.

Baker, S. A., Freeman, K., Luby-Phelps, K., Pazour, G. J. and Besharse, J. C. (2003). IFT20 links kinesin II with a mammalian intraflagellar transport complex that is conserved in motile flagella and sensory cilia. *J. Biol. Chem.* **278**, 34211-34218.

Buscher, D., Bosse, B., Heymer, J. and Ruther, U. (1997). Evidence for genetic control of *Sonic hedgehog* by Gli3 in mouse limb development. *Mech. Dev.* **62**, 175-182.

Chiang, C., Litingtung, Y., Lee, E., Young, K. E., Corden, J. L., Westphal, H. and Beachy, P. A. (1996). Cyclopia and defective axial patterning in mice lacking *Sonic hedgehog* gene function. *Nature* **383**, 407-413.

Chiang, C., Litingtung, Y., Harris, M. P., Simandl, B. K., Li, Y., Beachy, P. A. and Fallon, J. F. (2001). Manifestation of the limb prepattern: limb development in the absence of sonic hedgehog function. *Dev. Biol.* **236**, 421-435.

Chuang, P. T. and McMahon, A. P. (1999). Vertebrate Hedgehog signalling modulated by induction of a Hedgehog-binding protein. *Nature* **397**, 617-621.

Dai, P., Akimaru, H., Tanaka, Y., Maekawa, T., Nakafuku, M. and Ishii, S. (1999). Sonic Hedgehog-induced activation of the Gli1 promoter is mediated by GLI3. *J. Biol. Chem.* **274**, 8143-8152.

Ding, Q., Motoyama, J., Gasca, S., Mo, R., Sasaki, H., Rossant, J. and Hui, C. C. (1998). Diminished Sonic hedgehog signaling and lack of floor plate differentiation in Gli2 mutant mice. *Development* **125**, 2533-2543.

Goodrich, L. V., Milenkovic, L., Higgins, K. M. and Scott, M. P. (1997). Altered neural cell fates and medulloblastoma in mouse patched mutants. *Science* **277**, 1109-1113.

Han, Y. G., Kwok, B. H. and Kernan, M. J. (2003). Intraflagellar transport is required in Drosophila to differentiate sensory cilia but not sperm. *Curr. Biol.* **13**, 1679-1686.

Huangfu, D., Liu, A., Rakeman, A. S., Murcia, N. S., Niswander, L. and Anderson, K. V. (2003). Hedgehog signalling in the mouse requires intraflagellar transport proteins. *Nature* **426**, 83-87.

Hui, C. C. and Joyner, A. L. (1993). A mouse model of greig cephalopolysyndactyly syndrome: the extra-toesJ mutation contains an intragenic deletion of the *Gli3* gene. *Nat. Genet.* **3**, 241-246.

Ingham, P. W. and McMahon, A. P. (2001). Hedgehog signaling in animal development: paradigms and principles. *Genes Dev.* **15**, 3059-3087.

Izraeli, S., Lowe, L. A., Bertness, V. L., Good, D. J., Dorward, D. W., Kirsch, I. R. and Kuehn, M. R. (1999). The SIL gene is required for mouse embryonic axial development and left-right specification. *Nature* **399**, 691-694.

Jia, J., Tong, C. and Jiang, J. (2003). Smoothened transduces Hedgehog signal by physically interacting with Costal2/Fused complex through its C-terminal tail. *Genes Dev.* **17**, 2709-2720.

Knezevic, V., De Santo, R., Schughart, K., Huffstadt, U., Chiang, C., Mahon, K. A. and Mackem, S. (1997). *Hoxd-12* differentially affects preaxial and postaxial chondrogenic branches in the limb and regulates *Sonic hedgehog* in a positive feedback loop. *Development* **124**, 4523-4536.

Kraus, P., Fraidenraich, D. and Loomis, C. A. (2001). Some distal limb structures develop in mice lacking Sonic hedgehog signaling. *Mech. Dev.* **100**, 45-58.

Lee, C. S., Buttitta, L. and Fan, C. M. (2001). Evidence that the WNT-inducible growth arrest-specific gene 1 encodes an antagonist of sonic hedgehog signaling in the somite. *Proc. Natl. Acad. Sci. USA* **98**, 11347-11352.

Lefers, M. A., Wang, Q. T. and Holmgren, R. A. (2001). Genetic dissection of the Drosophila Cubitus interruptus signaling complex. *Dev. Biol.* **236**, 411-420.

Litingtung, Y. and Chiang, C. (2000). Specification of ventral neuron types is mediated by an antagonistic interaction between Shh and Gli3. *Nat. Neurosci.* **3**, 979-985.

Litingtung, Y., Dahn, R. D., Li, Y., Fallon, J. F. and Chiang, C. (2002). Shh and Gli3 are dispensable for limb skeleton formation but regulate digit number and identity. *Nature* **418**, 979-983.

Liu, A., Joyner, A. L. and Turnbull, D. H. (1998). Alteration of limb and brain patterning in early mouse embryos by ultrasound-guided injection of Shh-expressing cells. *Mech. Dev.* **75**, 107-115.

Liu, A., Losos, K. and Joyner, A. L. (1999). FGF8 can activate Gbx2 and transform regions of the rostral mouse brain into a hindbrain fate. *Development* **126**, 4827-4838.

Lum, L. and Beachy, P. A. (2004). The Hedgehog response network: sensors, switches, and routers. *Science* **304**, 1755-1759.

Lum, L., Zhang, C., Oh, S., Mann, R. K., von Kessler, D. P., Taipale, J., Weis-Garcia, F., Gong, R., Wang, B. and Beachy, P. A. (2003). Hedgehog signal transduction *via* Smoothened association with a cytoplasmic complex scaffolded by the atypical kinesin, Costal-2. *Mol. Cell* **12**, 1261-1274.

Matise, M. P., Epstein, D. J., Park, H. L., Platt, K. A. and Joyner, A. L. (1998). Gli2 is required for induction of floor plate and adjacent cells, but not most ventral neurons in the mouse central nervous system. *Development* **125**, 2759-2770.

McCarthy, R. A., Barth, J. L., Chintalapudi, M. R., Knaak, C. and Argraves, W. S. (2002). Megalin functions as an endocytic sonic hedgehog receptor. *J. Biol. Chem.* **277**, 25660-25667.

Morgan, B. A., Izpisua-Belmonte, J. C., Duboule, D. and Tabin, C. J. (1992). Targeted misexpression of Hox-4.6 in the avian limb bud causes apparent homeotic transformations. *Nature* **358**, 236-239.

Moyer, J. H., Lee-Tischler, M. J., Kwon, H. Y., Schrick, J. J., Avner, E. D., Sweeney, W. E., Godfrey, V. L., Cacheiro, N. L., Wilkinson, J. E. and Woychik, R. P. (1994). Candidate gene associated with a mutation causing recessive polycystic kidney disease in mice. *Science* **264**, 1329-1333.

Niswander, L. (2003). Pattern formation: old models out on a limb. *Nat. Rev. Genet.* **4**, 133-143.

Niswander, L. and Martin, G. R. (1992). Fgf-4 expression during gastrulation, myogenesis, limb and tooth development in the mouse. *Development* **114**, 755-768.

Ogden, S. K., Ascano, M., Jr, Stegman, M. A., Suber, L. M., Hooper, J. E. and Robbins, D. J. (2003). Identification of a functional interaction between the transmembrane protein Smoothened and the kinesin-related protein Costal2. *Curr. Biol.* **13**, 1998-2003.

Riddle, R. D., Johnson, R. L., Laufer, E. and Tabin, C. (1993). Sonic hedgehog mediates the polarizing activity of the ZPA. *Cell* **75**, 1401-1416.

Rosenbaum, J. L. and Witman, G. B. (2002). Intraflagellar transport. *Nat. Rev. Mol. Cell Biol.* **3**, 813-825.

Ruel, L., Rodriguez, R., Gallet, A., Lavenant-Staccini, L. and Therond, P. P. (2003). Stability and association of Smoothened, Costal2 and Fused with Cubitus interruptus are regulated by Hedgehog. *Nat. Cell Biol.* **5**, 907-913.

Sarpal, R., Todi, S. V., Sivan-Loukianova, E., Shirolikar, S., Subramanian, N., Raff, E. C., Erickson, J. W., Ray, K. and Eberl, D. F. (2003). Drosophila KAP interacts with the kinesin II motor subunit KLP64D to assemble chordotonal sensory cilia, but not sperm tails. *Curr. Biol.* **13**, 1687-1696.

Sasaki, H., Nishizaki, Y., Hui, C., Nakafuku, M. and Kondoh, H. (1999). Regulation of Gli2 and Gli3 activities by an amino-terminal repression domain: implication of Gli2 and Gli3 as primary mediators of Shh signaling. *Development* **126**, 3915-3924.

Sekimizu, K., Nishioka, N., Sasaki, H., Takeda, H., Karlstrom, R. O. and Kawakami, A. (2004). The zebrafish iguana locus encodes Dzip1, a novel zinc-finger protein required for proper regulation of Hedgehog signaling. *Development* **131**, 2521-2532.

te Welscher, P., Fernandez-Teran, M., Ros, M. A. and Zeller, R. (2002a). Mutual genetic antagonism involving GLI3 and dHAND prepatterns the vertebrate limb bud mesenchyme prior to SHH signaling. *Genes Dev.* **16**, 421-426.

te Welscher, P., Zuniga, A., Kuijper, S., Drenth, T., Goedemans, H. J., Meijlink, F. and Zeller, R. (2002b). Progression of vertebrate limb development through SHH-mediated counteraction of GLI3. *Science* **298**, 827-830.

Timmer, J., Johnson, J. and Niswander, L. (2001). The use of in ovo electroporation for the rapid analysis of neural-specific murine enhancers. *Genesis* **29**, 123-132.

Wang, B., Fallon, J. F. and Beachy, P. A. (2000). Hedgehog-regulated processing of Gli3 produces an anterior/posterior repressor gradient in the developing vertebrate limb. *Cell* **100**, 423-434.

Wang, Q. T. and Holmgren, R. A. (2000). Nuclear import of cubitus interruptus is regulated by hedgehog *via* a mechanism distinct from Ci stabilization and Ci activation. *Development* **127**, 3131-3139.

Wick, M. J., Ann, D. K. and Loh, H. H. (1995). Molecular cloning of a novel protein regulated by opioid treatment of NG108-15 cells. *Brain Res. Mol. Brain Res.* **32**, 171-175.

Wolff, C., Roy, S., Lewis, K. E., Schauerte, H., Joerg-Rauch, G., Kirn, A., Weiler, C., Geisler, R., Haffter, P. and Ingham, P. W. (2004). iguana encodes a novel zinc-finger protein with coiled-coil domains essential for Hedgehog signal transduction in the zebrafish embryo. *Genes Dev.* **18**, 1565-1576.

Yang, Y., Guillot, P., Boyd, Y., Lyon, M. F. and McMahon, A. P. (1998). Evidence that preaxial polydactyly in the Doublefoot mutant is due to ectopic Indian Hedgehog signaling. *Development* **125**, 3123-3132.

Zhang, Q., Murcia, N. S., Chittenden, L. R., Richards, W. G., Michaud, E. J., Woychik, R. P. and Yoder, B. K. (2003). Loss of the Tg737 protein results in skeletal patterning defects. *Dev. Dyn.* **227**, 78-90.